Odor Assessment of Automobile Interior Components Using Ion Mobility Spectrometry

Juan Li[1], Ricardo Gutierrez-Osuna[2], Ryan D. Hodges[1], Gail Luckey[3], Joel Crowell[3], Susan S. Schiffman[1] and H. Troy Nagle[1]

[1] Electrical & Computer Engineering, NC State University, Raleigh, NC, USA, jli35@ncsu.edu
[2] Computer Science & Engineering, Texas A&M University, College Station, TX, USA
[3] Materials Development, Hyundai Motor Group, Superior Township, MI, USA

***Abstract*—Evaluating and improving odors emitted from automobile interior parts can help automotive companies fulfill prospective customers' expectations of odor character and health impacts. Extending our previous work on machine-versus-human odor assessment for intact automobile cabin interiors, in this study we evaluated odors generated from individual interior parts using a human panel and ion mobility spectrometry (IMS). We used image processing to extract geometric features from IMS dispersion fields, and built predictive models for three odor assessment parameters (intensity, irritation, and pleasantness) by means of partial least squares regression. Using cross validation, we achieved statistically significant correlations in the range from 0.483 to 0.616 with a sample set of 48 interior automobile parts. These results support the feasibility of replacing a human panel by machine-olfaction for the assessment of odor quality of interior automobile parts.**

Keywords— automobile odors; machine olfaction; ion mobility spectrometry; odor assessment; partial least squares regression

I. INTRODUCTION

In addition to reliability and safety, odors quality has become an important factor in customers' preferences when they acquire new automobiles. Odors inside automobiles are complex mixtures of various volatile organic compounds (VOCs) that partly come from the materials of various interior parts. In order to improve customers' impressions of a manufacturer's automobile offerings, the odor (gas mixture) emitted from each part should be evaluated for its contribution to collective cabin odor. In this study we evaluated odors emanating from 10 parts from five different vehicle models provided by the Hyundai Motor Group.

Traditional machine olfaction systems are based on arrays of cross-selective sensors using gas sensing technologies, including metal oxide semiconductor (MOS), MOS field effect transistor (MOSFET), conducting polymer (CP), surface and bulk acoustic wave (SAW, BAW), fluorescence (FL), infrared (IR) absorption, and optics [1-3]. Because of the limited chemical selectivity of a single sensor, an array of gas sensors can expand the system's sensing range. Such a sensor array combined with pattern recognition methods constitutes a machine olfaction system, which is also called an electronic nose (e-nose). An e-nose can identify chemicals and predict sensory attributes of gas mixtures [4]. But the sensor array is usually selected to respond to specific gas mixtures. When the target gases are changed beyond the system's original design, the system will be inaccurate.

Ion mobility spectrometry (IMS) is an alternative technique to detect a wide variety of gases. This technique was developed for gas sensing in the early 1970s [5]. It is a portable and sophisticated chemical analyzer for detecting a wide range of organic chemicals [6]. IMS can monitor ambient air to detect target gases in real-time with a measuring resolution in parts per billion. IMS identifies analytes by their mobility according to molecules' size, mass, charge and shape, which enables measurement of a large range of analytes. Since many factors can affect the spectra, there are no commonly accepted standards for experimental conditions to reach optimal IMS performance. Finding odor-relevant information under different experimental conditions is the challenge when developing an IMS-based machine olfaction system.

In this study, we employed a Lonestar IMS by Owlstone, Inc., to examine odors generated from different automobile parts. Image processing methods were used to extract efficient odor-relevant information from acquired IMS spectra signals. Regression models based on selected features were built to predict three odor sensory parameters (intensity, irritation, and pleasantness) for the respective automobile parts. This paper is organized as follows. In Section II, the experimental setup and detailed procedures are introduced. Feature extraction methods are described in Section III, as well as regression models using partial least squares. Conclusions from the study are summarized in Section IV.

II. EXPERIMENTS

A. Samples

Odor can emanate from a variety of component parts comprising an automobile's interior cabin. Table I lists our selection of 10 types of parts (labeled from "a" to "j") from five different automobile models (labeled from "A" to "E"). The selected parts were: floor carpet, floor mat, headliner, instrument panel, rear package tray, cloth bolster for seat cover, cloth insert for seat cover, leather bolster for seat cover, leather insert for seat cover, and seat foam. Two of the models had no rear package tray, so a total of 48 samples were tested (each sample's identifying number is listed in Table I).

978-1-4799-8203-5/15/$31.00 ©2015 IEEE

TABLE I. AUTOMOBILE PART SAMPLE IDENTIFIERS

Sample No.	Vehicle Model				
	A	*B*	*C*	*D*	*E*
a. Floor carpet	9	23	37	34	42
b. Floor mat	44	11	25	22	8
c. Headliner	45	24	26	1	43
d. Instrument panel	32	7	13	10	31
e. Rear package tray	33	12	14	none	none
f. Cloth bolster for seat cover	15	48	18	46	16
g. Cloth insert for seat cover	3	36	6	17	4
h. Leather bolster for seat cover	39	47	38	5	40
i. Leather insert for seat cover	27	35	30	41	28
j. Seat foam	21	19	2	29	20

B. *Human Panels*

Our odor panel consisted of four trained evaluators. The detailed human panel training procedure can be found in [7, 8]. During the experiments, each panel member sniffed each of the 48 samples and rated it for intensity, irritation, and pleasantness. For each evaluating parameter, the panelists scored the odor using a standard scale from 0 to 8, where a rating of 0 denotes no intensity, no irritation and extremely pleasant, and a rating of 8 means maximal odor intensity, maximal irritation and extremely unpleasant; neutral pleasantness is rated as 4.

C. *Experimental Procedure*

A four-liter glass jar was used as the sample container. The jar had a custom Teflon disc fashioned as a cover with two ports, one for extracting headspace odor samples and the other resupplying odorless dry filtered clean air. Prior to each sample test, the jar's interior and exterior were cleaned using deionized water and ethyl alcohol (EtOH). This step removed any odor residues left in the jar during previous tests. The clean empty jar was sealed and placed in a heated oven at 80ºC for one hour. After removing the jar from the oven, a SKC pump was used to transfer the headspace gas from the jar to the Lonestar IMS. Three IMS measurements (each taking three minutes) were collected from the clean empty jar. These three measurements were used as background odor since some trace residues surviving our jar-cleaning process may have generated VOCs during the one-hour heating cycle. These background measurements were subtracted from the sample measurements during data processing to minimize interferences from such potential background odors.

Next, a representative piece from one of the 48 parts was placed inside the jar (typically cut in the shape of a small rectangular block ≈ 3"×4"×2"). The jar containing the sample piece was sealed and placed into an oven at 80ºC for two hours. Following heating, the sealed jar with the sample piece was removed from the oven and allowed to cool at room temperature for another hour. Then the four human panelists sniffed the odor from inside the jar by sliding the Teflon cover slightly to the side, attempting to minimize headspace dilution. Finally, the Lonestar IMS measured the odor sample after human panelists finished their evaluation. For each sample piece, the Lonestar IMS also acquired three measurements (each taking three minutes). This procedure was repeated for all 48 samples.

III. RESULTS AND DISCUSSION

A. *Lonestar Sample Data*

The Lonestar IMS uses field asymmetric IMS technology in which ions move under strong electronic field conditions. A Ni^{63} radiation source is employed by the Lonestar IMS to ionize the molecules in a pressurized air stream. This airstream transverses a conductive channel in which an alternating asymmetric electric field is applied along with a sweeping DC bias, which is swept as the amplitude of the alternating field is increased. Ions that reach the end of the channel (those that avoid colliding with the walls) generate a current proportional to the number of ions surviving the channel's electric field dynamics. A dispersion field matrix (DFM) for positive ions and negative ions respectively is the measured ion current as a function of applied DC bias and the amplitude of the applied asymmetric alternating electric field [9]. This leads to a unique identification for ions with the same mobility. The DC bias is swept from -6V to +6V in our experiments.

Positive and negative DFMs for one sample part are shown in Fig. 1. For different chemicals, the information shown in the positive and negative DFM may be different if they have different proton or electron affinity. In our measurements, each DFM has dimensions 51×512. These data dimensions can be compared to a typical e-nose instrument that might generate data sets with dimensions 16×30 (16 sensors sampled for 30 seconds) [10]. Therefore, finding a good feature extraction algorithm to reduce the Lonestar IMS dataset to a smaller number of highly related indicators of odor quality is even more important than for a typical e-nose instrument.

B. *Principal Components Analysis*

First, we apply principal components analysis (PCA), a commonly used e-nose feature extraction method, on our Lonestar DFM data. In particular, we employed "snapshot" PCA [8, 11]. This method projects an average of three preprocessed DFM measurements of each sample into independent directions based on their maximum variance matrix among all 48 samples. The eigenvector for each direction is calculated by a linear combination of all features to avoid inverting large matrices. For our dataset, the first three out of 48 principal components (PCs) capture more than 90% of the variance and were used for all subsequent processing. The correlation between these three PCs and human panel evaluation scores is shown in Table II. The highest correlation between the three PCs and the human panel evaluations is 0.403.

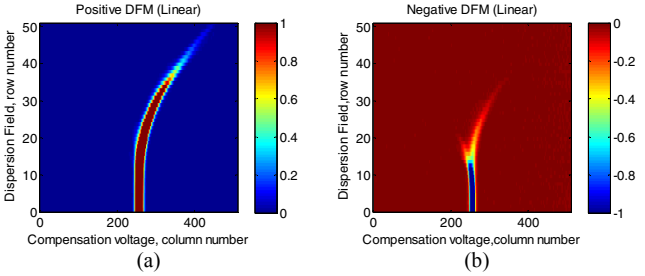

Fig. 1. DFM of one floor mat sample piece. (a) Positive DFM. (b) Negative DFM.

TABLE II. CORRELATION BETWEEN LONESTAR MEASUREMENTS AND HUMAN PANEL DATA

Principal Components of Lonestar Data	Human Panel Evaluation		
	Intensity	*Irritation*	*Pleasantness*
1	0.050	0.382	0.299
2	0.173	0.325	**0.403**
3	0.017	-0.041	0.073

Odor quality predictions, generated by principal components regression models based on these first three PCs, are correlated with human panel evaluation scores as –0.307 for intensity, 0.362 for irritation, and 0.287 for pleasantness after k-fold cross-validation (k = 48), with p-value are p=0.72, p<0.01, and p<0.01, respectively. These values are unacceptable, so we conclude that the PCA method does not extract highly relevant odor information.

C. Image Features

Based on these results, we decided to extract more relevant features using image processing techniques. As shown in Fig. 2, each row in a DFM can be viewed as a two-dimensional plot. In order to capture the spectra profile information of the DFM, we turned the positive and negative DFMs into binary images by setting a threshold (dashed line) with absolute value of 0.075 A.U. in Fig. 2, resulting in the binary images shown in Fig. 3. Then, we used MATLAB image processing toolbox [12] to extract the following features from each binary image:

1) Centroid

The centroid is the center of shape of the region of interest (in white pixels), and can be derived as

$$C_x = \frac{1}{N}\sum_{i=1}^{N} x_i \quad , \quad C_y = \frac{1}{N}\sum_{i=1}^{N} y_i \tag{1}$$

where (x_i, y_i) is the location of a white pixel and N is the total number of white pixels. The centroid of the selected floor mat odor sample is shown as a blue circle in Fig. 3.

2) Boundary

The boundary of the DFM binary image is detected using the Canny edge detection algorithm [13]. The Canny detection operator convolves the image with a symmetric two-dimensional Gaussian function, then differentiates the image along the normal to the edge direction to find the edge. With the same standard deviation σ for both directions x and y, a two-dimensional Gaussian function can be defined as:

$$G = \exp(-\frac{x^2 + y^2}{2\sigma^2}) \tag{2}$$

The direction n is oriented normal to the direction of an edge to be detected:

$$n = \frac{\nabla(G * I)}{|\nabla(G * I)|} \tag{3}$$

where I is the image data and $*$ denotes convolution. An edge point is defined to be a local maximum of the image I along direction n after the operator G applied. Therefore, the edge can be calculated based on:

$$\frac{\partial^2}{\partial n^2} G * I = 0 \tag{4}$$

3) Corner location

The corner locations in each DFM binary image are capable of representing the tip locations of branches, which are related to types of chemicals in the gas mixture. Consequently, an example of the eight corner locations of region of interest are chosen from the following points defined in Fig. 4: top-left, top-right, right-top, right-bottom, bottom-right, bottom-left, left-bottom, and left-top. The identified eight corner points in the selected sample are shown as green circles in Fig. 3.

4) Area

The definition of the area of an image is the total of all pixels in the region of interest [14]. In our binary DFM images, the value of all the points in the region of interest is one (white), and the others are all zero (black). Then the area of the region of interest will be a sum of all the ones.

5) Boxed area

This feature is the area of a rectangular box enclosing the region of interest. The location of the box area is defined by the x and y position of the box's lower-left corner. The area is represented by the length and width of the box. The benefit of this method is to extract concurrently the region location, dimension ratio, and area. The rectangular box for the example sample is shown in green in Fig. 3.

6) Perimeter

The perimeter feature is a commonly used image property to represent image characteristics in one dimension. The perimeter is related to the variation of the edge of a region, and may not be captured by area alone. The perimeter is calculated by examining the points in the margin of the region [14]. In our case, the perimeter is the number of white pixels adjacent to black pixels.

D. Partial Least Squares Regression Models

Various combinations of the above features were evaluated as independent variables in linear regression models to predict the three odor quality parameters. The number of data elements in each of the six image features for one DFM is summarized in Table III.

Top nine regression results using partial least squares (PLS) are shown in Table IV. Each of the nine regression models employed different feature combinations and was verified by k-fold cross-validation (k = 48). Models 2 to 9 used increasing numbers and combinations of the image processing features. This approach resulted in several image feature combinations that generated higher correlations between predicted and original human panel assessments than models generated by PCs or DFMs (Feature 1) directly. Note that Model 9 using all six of the image features produces the highest overall correlation. The p-values of Model 9 for all three odor-

evaluation parameters are less than 0.01. The number of latent variables used in Model 9 was 22 for intensity, 22 for irritation, and 18 for pleasantness. The signal-to-noise ratios are 1.28, 1.14 and 0.97, respectively.

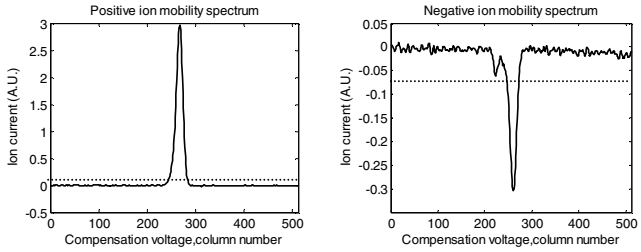

(a) (b)

Fig. 2. Ion mobility spectrum of one floor mat sample piece (DFM row 20). (a) Positive spectrum. (b) Negative spectrum.

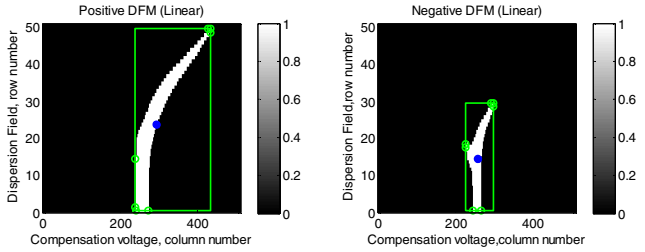

(a) (b)

Fig. 3. Image features of DFM binary images of one floor mat sample piece. (a) Positive binary DFM. (b) Negative binary DFM.

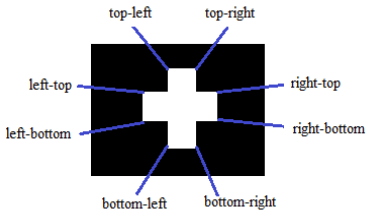

Fig. 4. Definition of corner location [12]

TABLE III. LIST OF SELECTED FEATURES FOR EACH DFM

No.	Features	Number of Data Elements
1	DFM	26112
2	Centroid	2
3	Boundary	26112
4	Corner location	16
5	Area	1
6	Boxed area	4
7	Perimeter	1

TABLE IV. CORRELATION BETWEEN PREDICTIONS AND ORIGINAL HUMAN PANEL DATA

Model No.	Features	Intensity	Irritation	Pleasantness
1	1	0.369	0.434	0.460
2	2	-0.192	0.360	0.432
3	2,4	0.431	0.519	0.407
4	2,3,6	-0.436	0.486	0.407
5	2,3,4,6	0.474	0.542	0.483
6	2,3,5,6	-0.124	0.523	0.420
7	2,5,6,7	0.327	0.507	0.409
8	2,3,5,6,7	0.326	0.500	0.418
9	2,3,4,5,6,7	**0.616**	**0.583**	**0.483**

IV. CONCLUSIONS

In order to help automobile companies satisfy customers' expectations for odor quality and health impact, we studied odors emanating from individual automobile component parts from within the vehicle's cabin. A Lonestar IMS was used as a VOC sensor. Feature extraction methods based on image processing were used to reduce the large dimensions of our IMS dataset. With *k*-fold cross-validation, the selected image features were shown to correlate with odor quality parameters assessed by a trained human panel. Predictive models based on combinations of image characteristics extracted from our IMS dataset performed better than models based on principal components derived from the same dataset. A PLS regression model using all six of our selected image features provided the best prediction of intensity, irritation and pleasantness. These results show potential for IMS-based machine olfaction as a cost-effective and consistent method to aid human panels in evaluating odor quality in the automobile industry.

REFERENCES

[1] A. D. Wilson, "Review of electronic-nose technologies and algorithms to detect hazardous chemicals in the environment," Procedia Technology, vol. 1, pp. 453-463, 2012.

[2] A. D. Wilson and M. Baietto, "Applications and advances in electronic-nose technologies," Sensors, vol. 9, pp. 5099-5148, 2009.

[3] A. D. Wilson and M. Baietto, "Advances in electronic-nose technologies developed for biomedical applications," Sensors, vol. 11, pp. 1105-1176, 2011.

[4] R. Gutierrez-Osuna, "Pattern analysis for machine olfaction: a review," IEEE Sensors Journal, vol. 2, pp. 189-202, 2002.

[5] W. Baether, S. Zimmermann, and F. Gunzer, "Pulsed ion mobility spectrometer for the detection of Toluene 2, 4-Diisocyanate in ambient Air," IEEE Sensors Journal, vol. 12, pp. 1748-1754, 2012.

[6] G. A. Eiceman, Z. Karpas, and H. H. Hill Jr, Ion mobility spectrometry: CRC press, 2013.

[7] T. C. Pearce, S. S. Schiffman, H. T. Nagle, and J. W. Gardner, Handbook of machine olfaction: electronic nose technology: John Wiley & Sons, 2006.

[8] J. Li, R. D. Hodges, R. Gutierrez-Osuna, G. Luckey, J. Crowell, S. S. Schiffman, and H. T. Nagle, "Odor assessment of automobile cabin air by machine olfaction," IEEE SENSORS 2014, Valencia, Spain, 2014, pp. 1726-1729.

[9] "Lonestar Ion Mobility Spectrometer," http://support.owlstonenanotech.com/entries/21639817-Introduction-to-FAIMS.

[10] R. Gutierrez-Osuna, S. Schiffman, and H. Nagle, "Correlation of sensory analysis with electronic nose data for swine odor remediation assessment," Proceedings of the 3rd European Congress on Odours, Metrology and Electronic Noses, 2001.

[11] L. Sirovich, "Turbulence and the dynamics of coherent structures. I-Coherent structures. II-Symmetries and transformations. III-Dynamics and scaling," Quarterly of applied mathematics, vol. 45, pp. 561-571, 1987.

[12] "MATLAB image processing toolbox," http://www.mathworks.com/help/images/ref/regionprops.html#bqkf8iq.

[13] J. Canny, "A computational approach to edge detection," IEEE Transactions on Pattern Analysis and Machine Intelligence, vol. PAMI-8, pp. 679-698, 1986.

[14] W. E. Snyder and H. Qi, Machine vision vol. 1: Cambridge University Press, 2004.